



## Spectral, Thermal and Antimicrobial Studies of Gamma Irradiated Potassium Diaquabis(Oxalato) Cobaltate(II)

T .A. JAYASHRI<sup>1\*</sup>, G. KRISHNAN<sup>2</sup> and K. VIJI<sup>1</sup>

<sup>1</sup>Department of Chemistry, University of Kerala, Thiruvananthapuram 695581, Kerala, India.

<sup>2</sup>Department of Chemistry, University College, Thiruvananthapuram 695034, Kerala, India.

\*Corresponding author E-mail: drjayashritaku@gmail.com

<http://dx.doi.org/10.13005/ojc/330144>

(Received: December 11, 2016; Accepted: February 08, 2017)

### ABSTRACT

Potassium diaquabis(oxalato)cobaltate(II) was prepared by reported method and characterized. The sample was irradiated with <sup>60</sup>Co gamma rays up to 900 kGy. Spectral (IR, UV-Visible), non-isothermal decomposition and antimicrobial properties of the complex were studied before and after irradiation. The bacterial strains screened were *E. Coli*, *K.pneumonia*, *B.Cereus*, and the fungal strains were *A.niger*, *A.fumigatus* and *Penicillium sp.* Notable changes in position and intensity of infrared bands after irradiation suggested hydrogen bonding and strong crosslinking in the irradiated sample. From UV spectra racah parameters were calculated before and after irradiation. Thermal decomposition was enhanced upon irradiation. Antibacterial properties of the complex were found to be decreased upon irradiation while antifungal properties were enhanced.

**Keywords:** Potassium diaquabis(oxalato)cobaltate(II);  $\gamma$ -irradiation; Spectral studies; Non-isothermal decomposition; Antimicrobial studies.

### INTRODUCTION

Gamma irradiation is known to increase the defect concentration in crystalline solids leading to chemical damage, displacements and extended lattice defects. Hence properties sensitive to defect concentration may be affected. Infrared studies of various irradiated materials including transition metal complexes are available in literature<sup>1-5</sup>. Fourier Transform Infrared (FT-IR) spectral studies of nickel amine complexes showed significant changes in position and intensity of characteristic bands after

irradiation<sup>3,4</sup>. Effect of irradiation on UV-Visible spectra of materials like glasses, polymers etc have also been studied<sup>6-8</sup>. However such studies in transition metal complexes are rare<sup>3,9,10</sup>. Effects of  $\gamma$ -irradiation on thermal decomposition of metal oxalates, bromates, etc., have been extensively studied<sup>11-13</sup>. Literature survey revealed that such studies in metal complexes are scarce<sup>14,15</sup>. All these studies showed that pre-treatment leads to enhancement of thermal decomposition. The present investigation proposes spectral (FT-IR, UV-Visible) and non-isothermal studies before and after

gamma irradiation of potassium diaquabis(oxalato) cobaltate(II).

Recently we have reported the enhanced antibacterial activity of gamma irradiated tris(1,2-diaminoethane)nickel(II) oxalate<sup>4</sup>. Hence the study also aims the antimicrobial activity of the titled compound before and after gamma irradiation.

### EXPERIMENTAL

The chemicals and reagents used were of AR grade, commercial cobalt (II) chloride hexahydrate and potassium oxalate monohydrate were used without purification. Potassium diaquabis(oxalato) cobaltate(II) dihydrate was prepared by known method<sup>16</sup>. The dried complex was stored over P<sub>2</sub>O<sub>5</sub> in vacuum desiccator. The complex was characterized by elemental analysis and spectral studies. The carbon and hydrogen contents in the obtained sample were determined by using Elementar Vario-

EL 111 CHNS analyzer. The complex was found to have octahedral geometry. The dried sample (100–120 mesh) sealed in pyrex ampoules were irradiated with <sup>60</sup>Coγ-ray to 300 kGy, 600 kGy and 900 kGy at constant intensity at a dose rate of 6 kGy/h. Irradiated samples were taken out, mixed uniformly and kept in desiccators over P<sub>2</sub>O<sub>5</sub>. Various studies were carried out within 1 week of irradiation. FT-IR and UV-Visible spectra of unirradiated and sample irradiated to 900 kGy were studied in the solid state. FT-IR spectra were recorded on a Perkin-Elmer 598 spectrometer in KBr pellets. UV-Visible spectra were recorded on SHIMADSU (model number 2550) UV-Visible spectrophotometer with 1cm matching quartz cells for the absorbance measurements. Non-isothermal studies of unirradiated and samples irradiated to varying doses (300 kGy, 600 kGy and 900 kGy) were carried out on a Perkin Elmer system. Heating rate was 10°C/min and the sample mass about 3 mg. Thermogram providing TG and DTG were simultaneously recorded in nitrogen atmosphere.

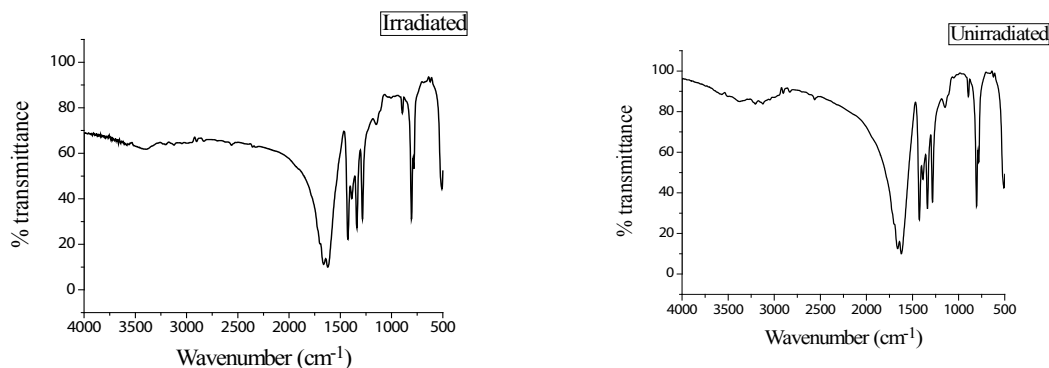


Fig.1: Infrared spectra of irradiated and unirradiated  $K_2[Co(C_2O_4)_2(H_2O)_2]$

Table: 1 Characteristic IR absorption bands for  $K_2[Co(C_2O_4)_2(H_2O)_2]$  and the corresponding assignments

Wavenumber (cm <sup>-1</sup> )	Assignment	Shift in peak position (cm <sup>-1</sup> )	% variation in intensity
Unirradiated 3205	900kGy 3188 $\nu_{asym}(O-H) + \nu_{sym}(O-H)$ or H bonding	17↓	15↑
1661 (s)	1666 $\nu_{asym}(O-C=O)$	5↑	-
1426 (s)	1426 $\nu_{sym}(C-O) + \nu(C-C)$	-	-
1147 (s)	1166 $\nu_{sym}(C-O) + \delta(O-C=O)$	19↑	-

The antibacterial activity of the unirradiated and irradiated samples (300 kGy, 600 kGy and 900 kGy) was studied by disc diffusion method using agar nutrient as medium. The bacterial strains screened were *E.Coli*, *K.Pneumonia*, *B.Cereus* and the fungal strains were *A.Niger*, *Fumigatus*, and *Penicilliumsp.* Measurements were carried out at three different concentrations. The standard chosen for bacteria was Nalidixic acid and that for fungus is Fluconazole.

**RESULTS AND DISCUSSION**

**Infrared spectra**

IR spectra of unirradiated and irradiated samples are depicted in figure (1). The peak assignments are presented in table (1). It can be seen that bands due to coordinated water appear at 3205 cm<sup>-1</sup> and 3188 cm<sup>-1</sup> respectively in the unirradiated and irradiated samples.  $\nu_{asym}$  (O-C=O) and  $\nu_{sym}$  (CO) +  $\nu$ (C-C) are observed in the regions 1670-1620 cm<sup>-1</sup> and 1430- 1100 cm<sup>-1</sup> in both the samples, i.e peak positions are almost unaffected. However the peak at 1147 cm<sup>-1</sup> in the unirradiated sample is shifted to a higher wave number 1166 cm<sup>-1</sup>.

Considerable change in intensity can be noticed in the region 3205-2850 cm<sup>-1</sup>. The peaks in the region 3300-3000 cm<sup>-1</sup> appears broad in the irradiated sample.

Hydrogen bonding or other secondary interactions between chemical groups usually cause a shift in peak position of the participating functional groups. Hydrogen bonding interactions usually move the stretching frequencies of the participating groups, e.g. O-H towards lower wave numbers usually with increased intensity and peak broadening<sup>17</sup>. Factors affecting the intensity of infrared peaks are dipole moment, concentration of molecules in the sample, transition probability etc.

Shift to lower wave number of  $\nu_{asym}$  (H<sub>2</sub>O) and  $\nu_{sym}$  (H<sub>2</sub>O) indicate weakening of the bonds. As the shift is accompanied by broadening and enhancement in intensity, hydrogen bonding or other secondary interactions between chemical groups can be expected in the irradiated sample. Shift to higher wave number  $\nu_{sym}$ (CO) +  $\delta$ (O-C=O) is suggestive of strengthening of the respective bond (table 1 and fig 1 ).

**Table: 2 Band assignments of unirradiated and irradiated K<sub>2</sub>[Co(C<sub>2</sub>O<sub>4</sub>)<sub>2</sub>(H<sub>2</sub>O)<sub>2</sub>]**

Sample	Band Assignments	Band position (cm <sup>-1</sup> )	
		Unirradiated	Irradiated
K <sub>2</sub> [Co(C <sub>2</sub> O <sub>4</sub> ) <sub>2</sub> (H <sub>2</sub> O) <sub>2</sub> ]	<sup>4</sup> T <sub>1g</sub> (F) → <sup>4</sup> T <sub>2g</sub>	13888	14044
	<sup>4</sup> T <sub>1g</sub> (F) → <sup>4</sup> A <sub>2g</sub>	18315	18181
	<sup>4</sup> T <sub>1g</sub> (F) → <sup>4</sup> T <sub>1g</sub> (P)	20283	20202

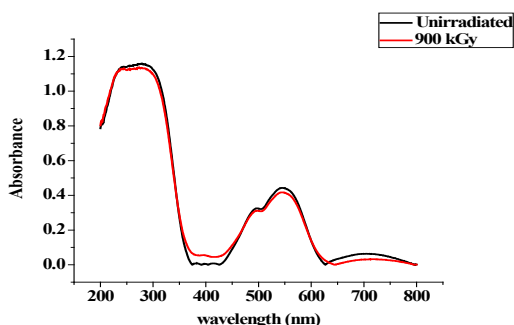


**Fig. 2: Electronic spectra of unirradiated and irradiated K<sub>2</sub>[Co(C<sub>2</sub>O<sub>4</sub>)<sub>2</sub>(H<sub>2</sub>O)<sub>2</sub>]**

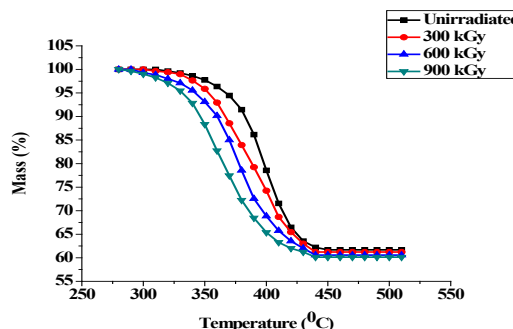


**Fig. 3: Thermal decomposition curves redrawn as percentage mass versus temperature curves for unirradiated and irradiated K<sub>2</sub>[Co(C<sub>2</sub>O<sub>4</sub>)<sub>2</sub>(H<sub>2</sub>O)<sub>2</sub>]**

### UV-Visible spectra

In the UV spectra of both unirradiated and irradiated samples four bands are seen. Respective band assignments are given in table (2). The intense band due to charge transfer at 276 nm in the unirradiated sample appears at 280 nm in the irradiated sample. The intensity of bands due to charge transfer as well as d-d transition is slightly lowered (fig 2).

The Racah parameters for unirradiated and irradiated samples were evaluated by graphical method. Results are given in table (3).

The energy difference between states having same multiplicity in a free transition metal ion is expressed in terms of Racah parameter, B. The value of this parameter is found to be less for a complexed metal ion implying changes in the position of energy levels. During complex formation, d-orbitals of metal ion overlap with the ligand orbitals, so that the metal–ligand bond become partially covalent. As a result the inter electronic repulsion within the d-orbitals decrease and B value is lowered. The reduction in the B value is related to the extent of metal-ligand covalency. For the complexed ion, the parameter is represented by B'. The ratio  $B'/B = \beta$ , known as nephelauxetic ratio, is a measure of covalency between the ligand and metal. Lower the value of  $\beta$ , greater is the covalency<sup>18</sup>. A number of factors such as vibrational phenomena, distortion to

lower symmetry, spin-orbit coupling and Jahn-Teller distortion can influence the electronic absorption spectra of transition metal complexes. Generally one or more of these factors operate in a metal complex so that the bands are broadened. Irradiation can affect the above mentioned factors causing further change in band widths.

If all the ligands in a hexa - coordinate complex are not the same the actual symmetry of the molecule will be lowered from Oh symmetry. But when the octahedral symmetry gets distorted, the orbital degeneracy of  $E_g$  and  $T_{2g}$  levels will be lifted and splitting of bands occurs. If the perturbation by the low symmetry component is small, splitting will be small, so that electronic transitions give rise to broad bands. The mechanism may also be operating in the complex. It is interesting to note that the different ligand field parameters are almost the same for unirradiated and irradiated  $K_2[Co(C_2O_4)_2(H_2O)_2]$  (table 3). This suggests that oxalate damage of cobalt complex is less. Crystal field strength is practically same for unirradiated and irradiated samples. So the changes in value are negligible.

### Thermal studies

#### Unirradiated sample

Thermal decomposition of potassium diaqua bis(oxalato)cobaltate(II) proceeds in a single stage. This stage commences at 582.2K and is completed at 723.4K. The peak temperature for this stage is 668K. Mass loss during this stage is 38.3% which can be attributed to the complete pyrolysis of the ligands (fig 3). Phenomenological data from non-isothermal analysis for the unirradiated sample is presented in (table 4). The reaction can be formulated as follows:

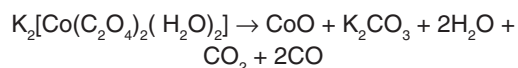


**Table 3: Spectral parameters of unirradiated and irradiated  $K_2[Co(C_2O_4)_2(H_2O)_2]$**

Sample	B' (cm <sup>-1</sup> )	LFSE (cm <sup>-1</sup> )	$\beta$
Unirradiated	870	9393	0.896
Irradiated	866	9378	0.892

**Table 4: Thermal decomposition data of unirradiated and irradiated  $K_2[Co(C_2O_4)_2(H_2O)_2]$**

Sample	%mass loss	Ti(K)	Tf(K)	Ts(K)	Taverage(K)
Unirradiated	38.30	582.2	723.4	668	652.8
300 kGy	38.77	575.3	722.7	655	648
600 kGy	39.43	572.1	713.5	648	644.4
900 kGy	39.86	563.4	712.2	645	637.8

### Irradiated sample

Irradiated samples also present single stage decomposition, but  $T_i$ ,  $T_f$  and  $T_s$  are found to be lowered. Percentage mass loss is also slightly varied (fig 3 and table 4).

In the sample irradiated to 300kGy decomposition starts at 575.3K and ends at 722.7K. Peak temperature for this stage is 655K and the observed mass loss is 38.77%. For the sample irradiated to 600kGy decomposition begins at 572.1K and ends at 713.5K. Peak temperature for this stage is 648K and the observed mass loss is 39.43%. In the sample irradiated to 900kGy decomposition starts at

563.4 and ends at 712.2K. Peak temperature for this stage is 645K and the observed mass loss is 39.86% (fig 3 and table 4).

The decomposition reactivity of crystalline solids depends upon the structural and energetic factors associated with chemical nature of the reactant, the lattice involved and the defects therein. Specifically defects determine the rate and mechanism of decomposition of a crystalline solid. Upon irradiation crystal defects are generated along with chemical damage. This situation enhances thermal decomposition.

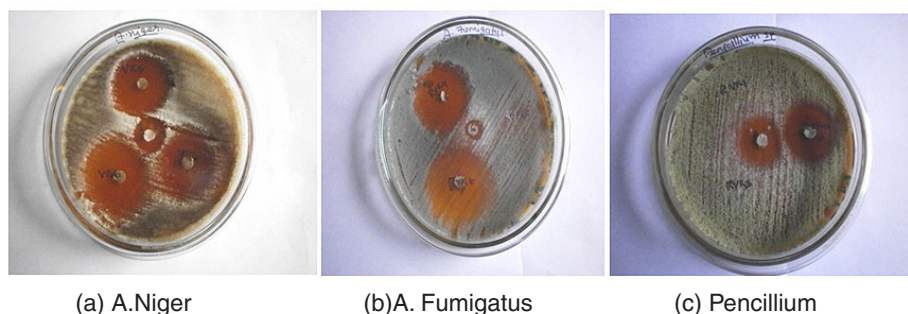


**Fig. 4: Antifungal activity of unirradiated and irradiated  $K_2[Co(C_2O_4)_2(H_2O)_2]$  (a) A.Niger (b)A. Fumigatus (c) Pencillium**

**Table 5: Lowering in  $T_i$ ,  $T_f$ ,  $T_s$  and percentage lowering in activation energy upon irradiation for  $K_2[Co(C_2O_4)_2(H_2O)_2]$**

Sample	$T_i(K)$	$T_f(K)$	$T_s(K)$	Percentage lowering in activation energy (CR)
300 kGy	6.9	0.7	13	14.39
600 kGy	10.1	9.9	20	15.51
900 kGy	18.8	11.2	23	26.46

**Table 6: Antibacterial activity of unirradiated and irradiated  $K_2[Co(C_2O_4)_2(H_2O)_2]$  Zone of inhibition (mm)**

Bacteria	<i>E.coli</i>	<i>K.pneumoniae</i>	<i>B.cereus</i>
Unirradiated	31	14	20
300 kGy	10	13	11
600 kGy	10	13	11
900 kGy	10	13	11

**Table 7: Antibacterial activity of unirradiated and irradiated  $K_2[Co(C_2O_4)_2(H_2O)_2]$  Zone of inhibition (mm) with concentration**

Bacteria	<i>E.coli</i>			<i>K.pneumoniae</i>			<i>B.cereus</i>		
Concentration ( $\mu g/mL$ )	50	100	150	50	100	150	50	100	150
Unirradiated	24	31	32	13	14	16	17	20	22
300 kGy	8	10	11	10	13	14	9	11	13

**Table 8: Antifungal activity of unirradiated and irradiated  $K_2[Co(C_2O_4)_2(H_2O)_2]$  Zone of inhibition (mm)**

Fungus	<i>A.niger</i>			<i>A.fumigatus</i>			<i>penicillium sp.</i>		
Concentration ( $\mu\text{g/mL}$ )	50	100	150	50	100	150	50	100	150
Unirradiated	6	8	-	9	12	-	9	11	-
300 kGy	11	15	-	10	13	-	10	12	-

**Table 9: Antifungal activity of unirradiated and irradiated  $K_2[Co(C_2O_4)_2(H_2O)_2]$  Zone of inhibition (mm) with concentration**

Fungus	<i>A.niger</i>	<i>A.fumigatus</i>	<i>penicillium sp</i>
Unirradiated	8	12	11
300 kGy	15	13	12
600 kGy	17	13	13
900 kGy	19	13	14

In the present study decomposition proceed in a single stage. From figure, it can be seen that unirradiated and irradiated samples follow the same decomposition pattern, but the reaction proceeds at a lower temperature. Lowering in  $T_i$ ,  $T_f$  and  $T_s$  of various samples for the single stage of decomposition is tabulated (Table 5). These results are in accordance with the previous reports on thermal decomposition studies of  $\gamma$ -irradiated cobalt complexes<sup>4,14</sup>.

$T_i$ ,  $T_f$  and  $T_s$  for the single stage decomposition are lowered upon irradiation, the effects being most pronounced for the sample irradiated to 900k Gy.

#### Antimicrobial studies

The results of antibacterial studies are presented in table (6, 7). It can be seen that activity towards *E.coli*, *B. Cereus* and *K.pneumonia* is decreased upon irradiation. Zone of inhibition is found to increase with increase in concentration of the test solution.

The results of antifungal studies are shown in table (8, 9). The irradiated samples show

enhanced activity towards all the three fungal strains (fig 4). Upon increasing the concentration of the test solution, inhibitory action initially increases but, is lost at highest concentration (150  $\mu\text{g/mL}$ ). Results suggest an optimum concentration for maximum activity. Irradiation leads to decreased antibacterial activity and improved antifungal activity.

Upon irradiation lattice defects are produced in addition to chemical damage. Radiation induces change in size and shape of particles. Surface defects and surface charges can affect the antimicrobial efficiency. It is also suggested that interesting applications can be achieved by controlling the defects, impurities, and the associated charge carriers<sup>19, 20</sup>.

#### CONCLUSION

IR spectral studies suggested hydrogen bonding and strong cross linking in the irradiated sample. Evaluation of racah parameters suggested negligible damage of the oxalate ligand. Thermal decomposition is enhanced by irradiation. Antimicrobial activity is sensitive to radiation treatment.

#### ACKNOWLEDGMENTS

The authors are thankful to the authorities of Central University, Pondicherry for providing facilities for  $\gamma$ -irradiation. Grateful acknowledgements are also rendered to STIC, Cochin,

CESS, Thiruvananthapuram and Department of Chemistry, University of Kerala for instrumental facilities.

## REFERENCES

1. Neenu Mary Thomas; Haisal Mathew; Sini Sebastian; Syamala Kumari, B.; Vinoy Thomas; Paulose, P.I.; Ancy Manuel. *Int. J. Sci. Res. Publ.* **2014**, *4*, 1-7.
2. Bashir Ahamed.; Raghuvanshi, S.K.; Siddhartha. ; Sharma, N.P.; Krishna, J.B.M.; Wahab, M.A. *Prog. Nanotech. Nanomat.* **2013**, *2*, 42-46.
3. Jayashri, T.A.; Krishnan, G.; Rema Rani, N. *Radiat. Eff. Def. Solid.* **2014**, *169*, 1019–1030.
4. Jayashri, T.A.; Krishnan, G.; Viji, K. *J. Radioanal. Nucl. Chem.* **2014**, *302*, 1021-1026.
5. Sumithra, I. S.; Jayashri, T. A.; Krishnan, G. *J. Radioanal. Nucl. Chem.* **2016**, *307*, 835–842.
6. Abou Sekkina, M. M.; El-Boraey, H. A. ; Aly, S. A. *J. Radioanal. Nucl. Chem.* **2014**, *300*, 867–872.
7. Bashir Ahmed.; Raghuvanshi, S. K.; Siddhartha.; Srivastava, A. K.; Krishna, J. B. M. Wahab, M. A. *Ind. J. Pure. Appl. Phy.* **2012**, *50*, 892-898.
8. Srinivasan, T.K.; Panigrahi, B.S.; Arora, A.K.; Venkatraman, B.; Ponraju, D. *Radia. Phys. Chem.* **2014**, *99*, 92–96.
9. Krishnan, G.; Jayashri, T.A.; Geetha Devi, K. *Radiat. Phys. Chem.* **2009**, *78*, 184–190.
10. Krishnan, G.; Jayashri, T.A.; Sudha, P. *Radiat. Phys. Chem.* **2009**, *78*, 933–938.
11. Abd El-Wahab, M.M.M.; Mahfouz, R.M. *Thermochim. Acta.* **1996**, *274*, 281–287.
12. Nayak, H.; Bhatta, D. *Thermochim. Acta.* **2000**, *362*, 99–105.
13. Samuel, J.; Surendran, A.; Culas, S. *J. Radioanal. Nucl. Chem.* **2013**, *295*, 53–61.
14. Krishnan, G.; Jayashri, T.A. *J. Radioanal. Nucl. Chem.* **2008**, *277*, 693–697.
15. Mousa, M.A.; Summan, A.M.; Al Sousi, G.N. *Thermochim. Acta.* **1990**, *165*, 23–29.
16. Agnieszka Chylewska.; Artur Sikorski.; Aleksandra D'bowska.; Lech Chmurzynski. *Cent. Eur. J. Chem.* **2013**, *11*, 8-15.
17. Randhawa, H.S. *Modern Molecular Spectroscopy.* **2003**, Macmillan.
18. Lever, A.D.P. *Inorganic electronic spectroscopy*, 2<sup>nd</sup> edition, **1984**, Elsevier, New York,
19. Padmavathy, N. ; Vijayaraghavan, R. *Sci. Technol. Adv. Mat.* **2008**, *9*, 1-7.
20. Lukas Schmidt-Mende. ; Judith L. MacManus-Driscoll. *Mater. Today.* **2007**, *10*, 40-48.